strains of *Salmonella typhimurium* YG7108, each coexpressing a form of human cytochrome P450 along with NADPH-cytochrome P450 reductase. Environ Mol Mutagen. 2001; 38: 339–46.

40 Thapliyal R, Maru GB. Inhibition of cytochrome P450 isozymes by curcumins *in vitro* and *in vivo*. Food Chem Toxicol. 2001; 39: 541–7.

41 Yang CS, Chhabra SK, Hong JY, Smith TJ. Mechanisms of inhibition of chemical toxicity and carcinogenesis by diallyl sulfide (DAS) and related compounds from garlic. J Nutr. 2001; 131: 1041S–5S.

42 Yamazaki Y, Fujita K, Nakayama K, Suzuki A, Nakamura K, Yamazaki H *et al.* Establishment of ten strains of genetically engineered *Salmonella typhimurium* TA1538 each co-expressing a form of human cytochrome P450 with NADPH-cytochrome P450 reductase sensitive to various promutagens. Mutat Res. 2004; 562: 151–62.

43 Conney AH, Buening MK, Pantuck EJ, Pantuck CB, Fortner JG, Anderson KE *et al.* Regulation of human drug metabolism by dietary factors. Ciba Found Symp. 1980; 76: 147–67.

44 Lasker JM, Huang MT, Conney AH. *In vitro* and *in vivo* activation of oxidative drug metabolism by flavonoids. J Pharmacol Exp Ther. 1984; 229: 162–70.

45 Li Y, Wang E, Patten CJ, Chen L, Yang CS. Effects of flavonoids on cytochrome P450-dependent acetaminophen metabolism in rats and human liver microsomes. Drug Metab Dispos. 1994; 22: 566–71.

Environmental and Molecular Mutagenesis 47:277–283 (2006)

In Vivo Mutagenesis in the Lungs of *gpt*-delta Transgenic Mice Treated Intratracheally With 1,6-Dinitropyrene

Akiko H. Hashimoto,[1] Kimiko Amanuma,[1] Kyoko Hiyoshi,[1,2] Hirohisa Takano,[1] Ken-ichi Masumura,[3] Takehiko Nohmi,[3] and Yasunobu Aoki[1]*

[1]*Research Center for Environmental Risk, National Institute for Environmental Studies, Ibaraki, Japan*

[2]*Graduate School of Comprehensive Human Sciences, University of Tsukuba, Ibaraki, Japan*

[3]*Division of Genetics and Mutagenesis, National Institute of Health Sciences, Tokyo, Japan*

1,6-Dinitropyrene (1,6-DNP) is a ubiquitous airborne pollutant found in diesel exhaust. In this study, mutagenesis was examined in the lungs of *gpt*-delta transgenic mice after intratracheal instillation of 0–0.1 mg 1,6-DNP. In addition, the 1,6-DNP-induced *gpt* mutation spectrum was compared with that of control mice. A single intratracheal injection of 0–0.05 mg 1,6-DNP resulted in significant dose-dependent increases in mutant frequency; the induced mutant frequency declined at the 0.1 mg dose. The average lung mutant frequencies at doses of 0.025, 0.05, and 0.1 mg 1,6-DNP were 2.9-, 4.1-, and 1.9-times higher than for control mice ($(0.50 \pm 0.16) \times 10^{-5}$). The major mutations induced by 1,6-DNP included G:C→A:T transitions, G:C→T:A transversions, and 1-base deletions. Among the G:C→A:T transitions isolated from 1,6-DNP-treated mice, five (at nucleotide positions 64, 110, 115, 116, and 418) were observed in four or more animals. These positions therefore are potential hotspots for 1,6-DNP mutation. The predominant frameshift mutations following 1,6-DNP treatment included single base pair deletions at G:C (9/13 = 69%). The results of this study indicate that 1,6-DNP is mutagenic for the lungs of mice. Environ. Mol. Mutagen. 47:277–283, 2006.

Key words: 1,6-dinitropyrene; *gpt*-delta transgenic mouse; 6-thioguanine selection

INTRODUCTION

Suspended particulate matter in diesel exhaust (DE) is a suspected cause of lung cancer and allergic respiratory disease, including bronchial asthma [Muranaka et al., 1986]. Various potent carcinogens and mutagens, such as polycyclic aromatic hydrocarbons (PAHs) and nitrated PAHs, have been identified in DE particles [Harris, 1983]. Some of the compounds in DE, for instance, benzo[*a*]pyrene (B[*a*]P) and dinitropyrenes (DNPs), are pulmonary carcinogens in animals [Tokiwa et al., 1984; Brightwell et al., 1986; Jeffrey et al., 1990]. Among the DNPs, 1,6-DNP-induced lung tumors were detected in 50% of BALB/c mice after 112 days of s.c. inoculation [Tokiwa et al., 1984]. Following intratracheal instillation of 1,6-DNP, 90–100% of hamsters developed lung carcinomas along with myeloid leukemias [Takayama et al., 1985]. Iwagawa et al. [1989] showed that direct pulmonary instillation of 1,6-DNP led to lung tumors in Fischer 344 rats, and mutations in K-*ras* codon 12 were observed in the tumors induced in rat lungs using a similar dosing protocol [Smith et al., 1997]. Also, DNA adduct formation and gene mutation were analyzed in F344 rats in which 1,6-DNP was directly administered to the lungs by implantation. A significant increase in *Hprt* gene mutations was detected in spleen T-lymphocytes [Smith et al., 1995].

Earlier in vitro assay results indicated that DNPs are potent mutagens. In the Salmonella mutation assay (Ames test), DNPs display strong mutagenicity without an exogenous metabolic activation system and predominantly induce frameshift-type mutations [Mermelstein et al., 1981; Sugimura and Takayama, 1983; Tokiwa et al.,

Grant sponsor: Japan Society for the Promotion of Sciences; Grant Number: 14207100.

*Correspondence to: Yasunobu Aoki, National Institute for Environmental Studies, 16-2 Onogawa, Tsukuba, Ibaraki 305-8506, Japan. E-mail: ybaoki@nies.go.jp

Received 22 September 2005; provisionally accepted 7 October 2005; and in final form 6 January 2006

DOI 10.1002/em.20204

Published online 17 February 2006 in Wiley InterScience (www.interscience.wiley.com).

1984]. Salmeen et al. [1984] showed that mono- and dinitro-PAHs, which include 1,3-, 1,6-, and 1,8-DNP, 1-nitropyrene, and 3- and 8-nitrofluoranthene, account for 30–40% of the direct bacterial mutagenic activity of extracts from DE particulate. 1,6-DNP and 1,8-DNP are activated by nitroreduction and *O*-acetylation in bacteria to form DNA adducts [Rosenkranz and Mermelstein, 1983]. Following a single i.p. injection of 1,6-DNP into mice, this mutagen binds to lung DNA as 1-*N*-(deoxyguanosin-8-yl) amino-6-nitropyrene [Delclos et al., 1987]. The same guanine adduct also was formed in rat lungs instilled with 1,6-DNP [Smith et al., 1995]. The in vivo mutagenicity and mutation spectrum of 1,6-DNP in the lung, a target organ for air pollutants, should be useful for elucidating its carcinogenic mechanism of action. Oral administration of 1,3-, 1,6-, and 1,8-DNP mixtures leads to in vivo mutagenicity in MutaMouse® [Kohara et al., 2002]. However, the mutagenic effects of 1,6-DNP in the lung remain to be determined.

To estimate the in vivo mutagenicity of 1,6-DNP in the lung, we used the *gpt*-delta transgenic mouse [Nohmi et al., 1996; Thybaud et al., 2003]. These mice carry a λ phage EG10 transgene that includes the guanine phosphoribosyltransferase (*gpt*) gene. When the rescued phages are infected into *E. coli* expressing Cre recombinase, phage DNA is converted into plasmids harboring a gene for chloramphenicol (Cm) resistance (*cat*) and the *gpt* gene. The *gpt* mutants are detected as colonies arising on plates containing Cm and 6-thioguanine (6-TG). In this study, the mutant frequency and mutation spectrum obtained from the lungs of *gpt*-delta mice were examined after intratracheal instillation of 1,6-DNP. Mutant frequency in the lung increased in the presence of 0-0.05 mg 1,6-DNP. The predominant mutations induced by 1,6-DNP were G:C→A:T transitions, G:C→T:A transversions, and single-base deletions at C:G sites. Specifically, *gpt* nucleotides no. 64, 110, 115, 116, and 418 appeared to be mutation hotspots.

MATERIALS AND METHODS

Treatment of Mice

Twelve male *gpt*-delta mice were obtained from Japan SLC (Shizuoka, Japan). These mice carry about 80 copies of λ EG10 DNA on chromosome 17 in a C57BL/6J background [Nohmi et al., 1996]. Doses of 1,6-DNP (Sigma–Aldrich Japan, Tokyo, Japan) dissolved in tricaprylin {$[CH_3(CH_2)_6COOCH_2]_2CHOCO(CH_2)_6CH_3$} (Sigma–Aldrich, St Louis, MO) were administered to each of three 9-week-old mice via a single intratracheal instillation. The animals were anesthetized with 4% halothane (Hoechst Japan, Tokyo, Japan) until the animal did not respond to a tactile stimulus. The animal was placed on a restraining board with linen threads to hold the mouth open. The 1,6-DNP solution was instilled into the trachea via a polyethylene tube [Takano et al., 2002; Hashimoto et al., 2005]. Two doses (0.025 and 0.05 mg) of 1,6-DNP were dissolved in 50 μl tricaprylin, while the 0.1 mg dose was dissolved in 100 μl tricaprylin. Three mice were treated with 50 μl tricaprylin alone as controls. Mice were killed 14 days after 1,6-DNP treatment, which a previous study [Suzuki et al., 1999] indicated was sufficient for mutant manifestation in the lung. Their lungs were removed, frozen in liquid nitrogen, and stored at −80°C until DNA isolation.

gpt Mutation Assay

The *gpt* assay was performed as described previously [Nohmi et al., 2000]. High molecular weight genomic DNA was extracted from the pooled lung tissue from each animal, using the RecoverEase DNA isolation kit (Stratagene, La Jolla, CA). λ EG10 phages were rescued using Transpack packaging extract (Stratagene). To convert phage DNA into plasmids, *E. coli* YG6020 expressing Cre recombinase was infected with phage. Bacteria were spread onto M9 salt plates containing Cm and 6-TG [Nohmi et al., 2000], and incubated for 72 hr at 37°C for selection of colonies harboring a plasmid carrying the Cm acetyltransferase (*cat*) gene and a mutated *gpt* gene. The 6-TG–resistant colonies were streaked onto selection plates for confirmation of the resistant phenotype. Cells were cultured in LB broth containing 25 μg/ml Cm at 37°C and collected by centrifugation. Bacterial pellets were stored at −80°C until sequencing analysis.

PCR and DNA Sequence Analysis of 6-TG-mutants

A 739-bp DNA fragment containing the *gpt* gene was amplified by PCR using primer-1 and primer-2, as described previously [Nohmi et al., 2000; Hashimoto et al., 2005]. The reaction mixture contained 5 pmol of each primer, and was 200 mM for each dNTP. PCR was performed using Ex *Taq* DNA polymerase (Takara Bio, Shiga, Japan) with a PTC-100 Thermal Cycler (MJ Research, Waltham, MA). The reaction mixture was incubated at 94°C for 4.5 min, followed by 30 cycles of 30 sec at 94°C, 30 sec at 58°C, and 1 min at 72°C. The last step was extended for 5 min at 72°C. After purification, amplified products were sequenced with a Big Dye Terminator v3.1 Cycle sequencing kit (Applied Biosystems, Foster City, CA) and an Applied Biosystems model 3730xl DNA analyzer. The sequencing oligonucleotides, primer-A and primer-C, are given in earlier reports [Nohmi et al., 2000; Hashimoto et al., 2005].

Statistical Analysis

All data are expressed as mean ± SD. The statistical significance of the mutant frequency data was analyzed using ANOVA and the Tukey post-hoc test. Data were considered statistically significant at $P < 0.05$. To evaluate the mutant frequency dose response, simple linear regression was performed. Mutational spectra were compared using the Adams–Skopek test [Adams and Skopek, 1987; Cariello et al., 1994].

RESULTS

1,6-DNP-Induced *gpt* Mutations in the Lung

To examine the mutagenic effects of 1,6-DNP in the lung, *gpt*-delta transgenic mice were exposed to increasing doses of 1,6-DNP (0.025, 0.05, and 0.1 mg/mouse) by intratracheal instillation (Fig. 1). The mutant frequency in the lungs of control mice was $(0.5 \pm 0.2) \times 10^{-5}$ (Table I). The mutant frequencies in control mice in this study were similar to those observed previously in several tissues of *gpt*-delta mice [Masumura et al., 1999, 2000, 2003; Hashimoto et al., 2005]. Single injections of 0.025, 0.05, and 0.1 mg 1,6-DNP resulted in 2.9-, 4.1-, and 1.9-

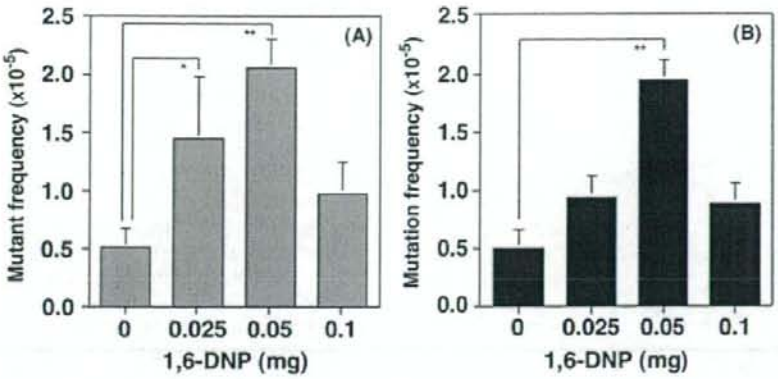

Fig. 1. 6-TG–resistant mutant frequency (A) and mutation frequency (B) in 1,6-DNP-treated *gpt*-delta mice. Data are presented as mean ± SD. Statistical significance was determined using ANOVA and Tukey tests. Significant differences between control and 1,6-DNP-induced groups are indicated (*$P < 0.05$, **$P < 0.01$).

TABLE I. Summary of Mutant and Mutation Frequencies in the Lungs of *gpt*-delta Mice After 1,6-DNP Treatment[a]

1,6-DNP amount (mg)	ID of animals	Number of colonies		Mutant frequency (10^{-5})	Average mutant frequency ± SD (10^{-5})	% independent mutations	Mutation frequency (10^{-5})	Average mutation frequency ± SD (10^{-5})
		Mutant	Total					
Control	1	3	441,600	0.68		100	0.68	
	2	3	643,200	0.47		100	0.47	
	3	3	828,000	0.36		100	0.36	
	Total	*9*	*1,912,800*		*0.50 ± 0.16*			*0.50 ± 0.16*
0.025	1	7	608,000	1.15		83	0.96	
	2	9	800,000	1.13		67	0.75	
	3	13	630,400	2.06		54	1.11	
	Total	*29*	*2,038,400*		*1.45 ± 0.53*[b]			*0.94 ± 0.18*
0.05	1	15	652,800	2.30		91	2.10	
	2	9	502,400	1.79		100	1.79	
	3	14	678,400	2.06		91	1.88	
	Total	*38*	*1,833,600*		*2.05 ± 0.25*[c]			*1.92 ± 0.15*[c]
0.1	1	12	953,600	1.26		83	1.05	
	2	7	1,000,000	0.70		100	0.70	
	3	5	536,000	0.93		100	0.93	
	Total	*24*	*2,489,600*		*0.96 ± 0.28*			*0.89 ± 0.18*

[a]Statistical significance was determined using ANOVA test and Tukey test. Significant differences between the control and 1,6-DNP treated groups are indicated.
[b]$P < 0.05$.
[c]$P < 0.01$.

fold increases in mutant frequency ($(1.5 \pm 0.5) \times 10^{-5}$, $(2.1 \pm 0.3) \times 10^{-5}$, and $(1.0 \pm 0.3) \times 10^{-5}$) and 1.9-, 3.8-, and 1.8-fold increases in mutation frequency ($(0.9 \pm 0.2) \times 10^{-5}$, $(1.9 \pm 0.2) \times 10^{-5}$, and $(0.9 \pm 0.2) \times 10^{-5}$), compared with that in control mice, respectively. Mutant frequency was significantly increased at doses of 0.025 and 0.05 mg 1,6-DNP, but not at a dose of 0.1 mg 1,6-DNP. The mutation frequencies in these mice, calculated by correcting the mutant frequencies for the independence of the mutants determined by DNA sequencing (see below), are also shown in Table I and Figure 1.

Characteristics of the *gpt* Mutant Spectrum in 1,6-DNP-Treated Mice

To determine the mutation spectrum induced by 1,6-DNP in the lung, 99 *gpt* mutants from the lungs of treated and control mice were subjected to DNA sequencing analysis (Table II, Fig. 2). G:C→A:T transitions, G:C→T:A transversions, and 1-base deletions were the major mutations induced by 1,6-DNP as shown in Figure 2, which shows the mutant frequency in the treatment groups associated with each type of mutation. In the 1,6-DNP treated group, 47% of the mutations (36 out of 77 mutants) were

TABLE II. Classification of *gpt* Mutations From the Lungs of Control and 1,6-DNP-Treated Mice[a]

Type of mutation in the *gpt* gene	Control[b]		1,6-DNP total[c]		1,6-DNP (mg)					
					0.025		0.05		0.1	
	Total/ independent	%/% independent	Total/ independent	%/% independent	Total/ independent	%/% independent	Total/ independent	%/% independent	Total/ independent	%/% independent
Base substitution										
Transition										
G:C→A:T (CpG site)	10/10 (3/3)	45/48	36/27 (21/13)	47/43	13/7 (9/4)	46/39	13/12 (6/5)	46/46	10/8 (6/4)	48/42
A:T→G:C	2/2	9/10	6/5	8/8	3/2	11/11	1/1	4/4	2/2	10/11
Transversion										
G:C→T:A	4/4	18/19	13/11	17/17	6/4	21/22	5/5	18/19	2/2	10/11
G:C→C:G	4/3	18/14	3/3	4/5	0	0	1/1	4/4	2/2	10/11
A:T→T:A	0	0	1/1	1/2	1/1	4/6	0	0	0	0
A:T→C:G	0	0	2/2	3/3	1/1	4/6	0	0	1/1	5/5
Deletion										
1-base	2/2	9/10	13/12	17/19	2/2	7/11	7/6	25/23	4/4	19/21
Insertion	0	0	3/2	4/3	2/1	7/6	1/1	4/4	0	0
Total	*22/21*	*100*	*77/63*	*100*	*28/18*	*100*	*28/26*	*100*	*2119*	*100*

[a]Independent mutations were isolated no more than once from any individual mouse.
[b]Control mutations are the sum of the mutations obtained from control animals in this study plus the mutations obtained from control animals in a previous study [Hashimoto et al., 2005]. The numbers of each type of mutation in control animals from this study were obtained from Table III.
[c]Mutations combined from all treatment doses.

G:C→A:T transitions, while 17% (13/77) were G:C→T:A transversions together with an equal percentage of 1-base deletions. In control mice, 78% (7/9) of the total mutations were G:C→A:T transitions. To increase the number of control mutants used for comparison, 9 mutants from this study were combined with 13 control lung mutants isolated from a previous study performed analogously to this one [Hashimoto et al., 2005], and this pooled mutant spectrum is used for the data shown in Table II and the mutant frequency distribution shown in Figure 2. There were no significant differences between spectra of the 22 control mutations and 77 total 1,6-DNP-induced mutations (Table II) ($P = 0.39$, Adams–Skopek test).

The *gpt* mutations isolated from 1,6-DNP-treated mice are listed in Table III. Among the G:C→A:T transitions isolated from treated mice, five (at nucleotides 64, 110, 115, 116, and 418) were observed in four or more mice. These positions are therefore potential hotspots for 1,6-DNP mutations: however, no significant differences were observed between the positions of the control mutations isolated in this study and the positions of the 1,6-DNP mutations ($P = 0.61$, Adams–Skopek test). There were also no significant differences between the positions of the 22 control lung mutations pooled from this study and our previous study [Hashimoto et al., 2005] and the 77 1,6-DNP-induced mutations ($P = 0.08$, Adams–Skopek test). The predominant frameshift mutation after 1,6-DNP treatment was single base-pair deletions at G:C (9/13 = 69%). Seventy-seven percent of 1-base deletions (10/13) occurred in run sequences, and there were no hotspots for 1-base deletions.

DISCUSSION

DNPs are recognized as potent environmental mutagens. Moreover, 1,6-DNP is a carcinogen in experimental animals [Tokiwa et al., 1984]. Using the Ames test, 43% of the direct mutagenicity of diesel particulate extracts was estimated to be due to contaminant DNPs [Nakagawa et al., 1983]. A 1,3-, 1,6-, and 1,8-DNP mixture was mutagenic in the liver, lung, colon, stomach, and bone marrow after intragastric injection in MutaMouse [Kohara et al., 2002]. However, little is known about the mechanism of in vivo mutagenesis by DNP.

To evaluate the mutagenicity of 1,6-DNP under exposure conditions appropriate for an air pollutant, the compound was administered intratracheally to *gpt*-delta mice. Treatment with 0–0.05 mg of this compound led to a linear increase in mutant and mutation frequency (Fig. 1), as shown previously with 0–2 mg B[*a*]P [Hashimoto et al., 2005]. The in vivo mutagenic potency (induced mutant frequency per amount of compound administered) for 1,6-DNP was 32×10^{-5} per mg, which was 13 times higher than that of B[*a*]P (2.4×10^{-5} per mg) [Hashimoto et al., 2005], indicating that 1,6-DNP was a

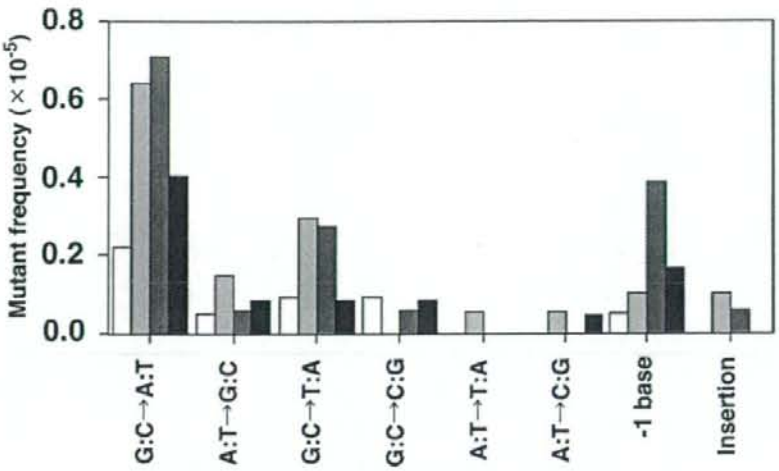

Fig. 2. Comparison of 1,6-DNP-induced and control mutation spectra in *gpt*-delta mice. White bar, control; light gray bar, 0.025 mg; dark gray bar, 0.05 mg; black bar, 0.1 mg. The analysis shown for control mutations is based on data combined from control animals in this study plus control animals from a previous study [Hashimoto et al., 2005].

more potent mutagen for the lung than B[*a*]P. However, the frequency was decreased at the highest dose (0.1 mg 1,6-DNP) to a lower level than that observed with 0.05 mg 1,6-DNP. We do not have any direct evidence to explain the decline in mutant frequency at high doses of 1,6-DNP in mice. Haugen et al. [1986] reported that unscheduled DNA synthesis, an index of excision repair in Clara cells and alveolar type-II cells, increased dose-dependently at low concentrations of 1,6-DNP, but decreased at high doses. This observation suggests that DNA adduct formation with 1,6-DNP is suppressed at high doses. Also, the amount of DNA adducts in 1,6-DNP-instilled rat lungs increased dose-dependently at low doses, but reached saturation at high doses [Smith et al., 1995]. The level of the 1,6-DNP-DNA adduct in lungs may be low at a dose of 0.1 mg 1,6-DNP, resulting in the lower mutant frequency. Finally it cannot be ruled out that cell proliferation in mice treated with 0.1 mg 1,6-DNP may not have been enough to fix the mutations because of the cytotoxicity of 1,6-DNP at high doses.

Our results indicate that G:C→A:T transitions, G:C→T:A transversions, and 1-base deletions are the major mutations induced by 1,6-DNP in the lung. On the other hand, Kohara et al. [2002] demonstrated that following the administration of DNP mixtures, the incidence of G:C→T:A transversions (43%) was higher than that of G:C→A:T transitions (22%) in the colon. Thus, the mutation spectrum of 1,6-DNP in the lung was different from the spectrum induced by the mixture of 1,3-, 1,6-, and 1,8-DNP in the colon. The metabolic reduction of 1,3-DNP and 1-nitropyrene was reported to be less extensive than that of 1,6- or 1,8-DNP, suggesting that the reduction pathways are distinct between these nitro-PAHs [Djuric et al., 1986]. Reduction as well as *O*-acetylation are important in determining the extent of DNA binding by 1,6- and 1,8-DNP in vivo [IPCS, 2003]. 1,6- and 1,8-DNP form *N*-(deoxyguanosin-8-yl)-1-amino-6-nitropyrene (dG-C8-1-amino-6-NP) and *N*-(deoxyguanosin-8-yl)-1-amino-8-nitropyrene (dG-C8-1-amino-8-NP) adducts, respectively [Smith et al., 1995; IPCS, 2003], while the adducts of 1,3-DNP have not been determined. We propose that differences in DNA adduct formation contribute to the variations in mutant spectra between 1,6-DNP and the 1,3-, 1,6-, and 1,8-DNP mixture.

Smith et al. [1997] reported that 1,6-DNP-induced lung tumors contain mutated K-*ras*. Among 20 specimens, 5 mutations in K-*ras* codon 12 (4 GGT to TGT transversions and 1 GGT to GAT), and 9 mutations in *p*53 exons 5–8 (8 substitutions at G:C base pairs and 1 deletion) were identified. These substitutions are consistent with the formation of dG adducts by 1,6-DNP. In our experiments, 1,6-DNP mainly induced substitutions in G:C pairs (61/77 = 79%), similar to the K-*ras* and *p*53 mutations in lung tumors.

Interestingly, we showed in an earlier report that the predominant mutations in the lungs of Big Blue rats exposed to 6 mg/m^3 DE for 1 month were G:C→A:T and A:T→G:C transitions [Sato et al., 2000]. The major mutations identified in the lungs of *gpt*-delta mice following exposure to 3 mg/m^3 DE for 3 months were G:C→A:T transitions (unpublished results, Hashimoto

TABLE III. DNA Sequence Analysis of *gpt* Mutation Obtained From the Lung of Control and 1,6-DNP-Treated *gpt*-delta Mice

Type of mutation in the *gpt* gene	Nucleotide	Sequence change	Site	Amino acid change	Number				
					Control all	1,6-DNP all	0.025 mg of 1,6-DNP	0.05 mg of 1,6-DNP	0.1 mg of 1,6-DNP
Base substitution									
Transition									
G:C→A:T	26	tGg→tAg		Trp→Stop		1		1	
	64	Cga→Tga	CpG	Arg→Stop	1	5[a]	1	2[b]	2[b]
	92	gGc→gAc		Gly→Asp		1		1	
	110	cGt→cAt	CpG	Arg→His	1	12[c]	6	3[b]	3
	115	Ggt→Agt	CpG	Gly→Ser		4[c]	2[b]	1	1
	116	gGt→gAt		Gly→Asp		4[c]	1	2[b]	1
	128	gGt→gAt		Gly→Asp	1				
	401	tGg→tAg		Trp→Stop	1	1			1
	402	tgG→tgA		Trp→Stop		1			1
	406	Gaa→Aaa		Glu→Lys		2[b]		2[b]	
	417	tgG→tgA		Trp→Stop	1				
	418	Gat→Aat		Asp→Asn	2[b]	5[c]	3[b]	1	1
A:T→G:C	56	cTc→cCc		Leu→Pro		1			1
	149	cTg→cCg		Leu→Pro		1	1		
	275	gAt→gGt		Asp→Gly		2	2		
	419	gAt→gGt		Asp→Gly		2[b]		1	1
Transversion									
G:C→T:A	59	gCa→gAa		Ala→Glu		1			1
	115	Ggt→Tgt	CpG	Gly→Cys		1		1	
	140	gCg→gAg	CpG	Ala→Glu		1		1	
	244	Gaa→Taa	CpG	Glu→Stop	1				
	262	Gat→Tat		Asp→Tyr		2[b]	2[b]		
	287	aCt→aAt		Thr→Asn		3	3		
	402	tgG→tgT		Trp→Cys		1		1	
	406	Gaa→Taa		Glu→Stop		2[b]	1	1	
	413	cCg→cAg	CpG	Pro→Gln		1			1
	418	Gat→Tat		Asp→Tyr		1		1	
G:C→C:G	131	gCg→gGg	CpG	Ala→Gly		1		1	
	206	cGc→cCc	CpG	Arg→Pro		1			1
	413	cCg→cGg	CpG	Pro→Arg		1			1
A:T→T:A	10	Aaa→Taa		Lys→Stop		1	1		
A:T→C:G	106	Agc→Cgc		Ser→Arg		1			1
	254	aTc→aGc		Ile→Ser		1	1		
Deletion									
1-base	8–12	gAAAAAt→gAAAAt				1		1	
	32	aTg→ag				1		1	
	97	tAt→tt				1			1
	115–116	cGGt→cGt				1		1	
	126–128	cGGGt→cGGt				1		1	
	170–171	aCCg→aCg				1	1		
	237	gCg→gg				1			1
	278–279	aCCg→aCg				1			1
	315–318	cAAAAg→cAAAg				1	1		
	358–359	tCCg→tCg				2		2	
	416–418	tGGGa→tGGa			1	1		1	
	423–425	tGGGc→tGGc				1			1
Insertion									
	291	cg→cAg				2	2		
	255	cg→cGTTATTGATGACCTg				1		1	

[a]Mutation found in five different mice.
[b]Mutation found in two different mice.
[c]Mutation found in four different mice.

et al.). As observed in DE-exposed lungs, G:C→A:T transition was the major base substitution (47%, 36 out of 77 mutants) induced by 1,6-DNP (Fig. 2), while G:C→T:A transversions were the predominant base substitution in B[*a*]P-instilled lungs of *gpt*-delta mice [Hashimoto et al., 2005]. Our results provide useful information on the in vivo mutations induced by 1,6-DNP in the lung.

ACKNOWLEDGMENTS

The authors thank Dr. Hiroaki Shiraishi, Dr. Michi Matsumoto, and Dr. Wakae Maruyama for support and advice.

REFERENCES

Adams WT, Skopek TR. 1987. Statistical test for the comparison of samples from mutational spectra. J Mol Biol 194:391–396.

Brightwell J, Fouillet X, Cassano-Zoppi AL, Gatz R, Duchosal F. 1986. Neoplastic and functional changes in rodents after chronic inhalation of engine exhaust emissions. Dev Toxicol Environ Sci 13: 471–485.

Cariello NF, Piegorsch WW, Adams WT, Skopek TR. 1994. Computer program for the analysis of mutational spectra: Application to *p53* mutations. Carcinogenesis 15:2281–2285.

Delclos KB, Walker RP, Dooley KL, Fu PP, Kadlubar FF. 1987. Carcinogen-DNA adduct formation in the lungs and livers of preweanling CD-1 male mice following administration of [^{3}H]-6-nitrochrysene, [^{3}H]-6-aminochrysene, and [^{3}H]-1,6-dinitropyrene. Cancer Res 47:6272–6277.

Djuric Z, Potter DW, Heflich RH, Beland FA. 1986. Aerobic and anaerobic reduction of nitrated pyrenes in vitro. Chem Biol Interact 59:309–324.

Harris JE. 1983. Diesel emission and lung cancer. Risk Anal 3:83–100.

Hashimoto AH, Amanuma K, Hiyoshi K, Takano H, Masumura K, Nohmi T, Aoki Y. 2005. In vivo mutagenesis induced by benzo[*a*]pyrene instilled into the lung of *gpt* delta transgenic mice. Environ Mol Mutagen 45:365–373.

Haugen A, Aune T, Deilhaug T. 1986. Nitropyrene-induced DNA repair in Clara cells and alveolar type-II cells isolated from rabbit lung. Mutat Res 175:259–262.

IPCS (International Programme on Chemical Safety). 2003. Selected nitro- and nitro-oxy-polycyclic aromatic hydrocarbons.Environmental health criteria 229. Geneva:World Health Organization. pp 161–164.

Iwagawa M, Maeda T, Izumi K, Otsuka H, Nishifuji K, Ohnishi Y, Aoki S. 1989. Comparative dose-response study on the pulmonary carcinogenicity of 1,6-dinitropyrene and benzo[*a*]pyrene in F344 rats. Carcinogenesis 10:1285–1290.

Jeffrey AM, Santella RM, Wong D, Hsieh LL, Heisig V, Doskocil G, Ghayourmanesh S. 1990. Metabolic activation of nitropyrenes and diesel particulate extracts. Res Rep Health Eff Inst 34:1–30.

Kohara A, Suzuki T, Honma M, Oomori T, Ohwada T, Hayashi M. 2002. Dinitropyrenes induce gene mutations in multiple organs of the lambda/*lac*Z transgenic mouse (Muta Mouse). Mutat Res 515:73–83.

Masumura K, Matsui M, Katoh M, Horiya N, Ueda O, Tanabe H, Yamada M, Suzuki H, Sofuni T, Nohmi T. 1999. Spectra of *gpt* mutations in ethylnitrosourea-treated and untreated transgenic mice. Environ Mol Mutagen 34:1–8.

Masumura K, Matsui K, Yamada M, Horiguchi M, Ishida K, Watanabe M, Wakabayashi K, Nohmi T. 2000. Characterization of mutations induced by 2-amino-1-methyl-6-phenylimidazo[4,5-*b*]pyridine in the colon of *gpt* delta transgenic mouse: Novel G:C deletions beside runs of identical bases. Carcinogenesis 21:2049–2056.

Masumura K, Totsuka Y, Wakabayashi K, Nohmi T. 2003. Potent genotoxicity of aminophenylnorharman, formed from non-mutagenic norharman and aniline, in the liver of *gpt* delta transgenic mouse. Carcinogenesis 24:1985–1993.

Mermelstein R, Kiriazides DK, Butler M, McCoy EC, Rosenkranz HS. 1981. The extraordinary mutagenicity of nitropyrenes in bacteria. Mutat Res 89:187–196.

Muranaka M, Suzuki S, Koizumi K, Takafuji S, Miyamoto T, Ikemori R, Tokiwa H. 1986. Adjuvant activity of diesel-exhaust particulates for the production of IgE antibody in mice. J Allergy Clin Immunol 77:616–623.

Nakagawa R, Kitamori S, Horikawa K, Nakashima K, Tokiwa H. 1983. Identification of dinitropyrenes in diesel-exhaust particles. Their probable presence as the major mutagens. Mutat Res 124:201–211.

Nohmi T, Katoh M, Suzuki H, Matsui M, Yamada M, Watanabe M, Suzuki M, Horiya N, Ueda O, Shibuya T, Ikeda H, Sofuni T. 1996. A new transgenic mouse mutagenesis test system using Spi$^-$ and 6-thioguanine selections. Environ Mol Mutagen 28:465–470.

Nohmi T, Suzuki T, Masumura K. 2000. Recent advances in the protocols of transgenic mouse mutation assays. Mutat Res 455:191–215.

Rosenkranz HS, Mermelstein R. 1983. Mutagenicity and genotoxicity of nitroarenes. All nitro-containing chemicals were not created equal. Mutat Res 114:217–267.

Salmeen IT, Pero AM, Zator R, Schuetzle D, Riley TL. 1984. Ames assay chromatograms and the identification of mutagens in diesel particle extracts. Environ Sci Technol 18:375–382.

Sato H, Sone H, Sagai M, Suzuki KT, Aoki Y. 2000. Increase in mutation frequency in lung of Big Blue rat by exposure to diesel exhaust. Carcinogenesis 21:653–661.

Smith BA, Fullerton NF, Heflich RH, Beland FA. 1995. DNA adduct formation and T-lymphocyte mutation induction in F344 rats implanted with tumorigenic doses of 1,6-dinitropyrene. Cancer Res 55:2316–2324.

Smith BA, Manjanatha MG, Pogribny IP, Mittelstaedt RA, Chen T, Fullerton NF, Beland FA, Heflich RH. 1997. Analysis of mutations in the K-*ras* and *p53* genes of lung tumors and in the *hprt* gene of 6-thioguanine-resistant T-lymphocytes from rats treated with 1,6-dinitropyrene. Mutat Res 379:61–68.

Sugimura T, Takayama S. 1983. Biological actions of nitroarenes in short-term tests on *Salmonella*, cultured mammalian cells and cultured human tracheal tissues: Possible basis for regulatory control. Environ Health Perspect 47:171–176.

Suzuki T, Itoh S, Nakajima M, Hachiya N, Hara T. 1999. Target organ and time-course in the mutagenicity of five carcinogens in Muta-Mouse: A summary report of the second collaborative study of the transgenic mouse mutation assay by JEMS/MMS. Mutat Res 444:259–268.

Takano H, Yanagisawa R, Ichinose T, Sadakane K, Inoue K, Yoshida S, Takeda K, Yoshino S, Yoshikawa T, Morita M. 2002. Lung expression of cytochrome P450 1A1 as a possible biomarker of exposure to diesel exhaust particles. Arch Toxicol 76:146–151.

Takayama S, Ishikawa T, Nakajima H, Sato S. 1985. Lung carcinoma induction in Syrian golden hamsters by intratracheal instillation of 1,6-dinitropyrene. Jpn J Cancer Res 76:457–461.

Thybaud V, Dean S, Nohmi T, de Boer J, Douglas GR, Glickman BW, Gorelick NJ, Heddle JA, Heflich RH, Lambert I, Martus HJ, Mirsalis JC, Suzuki T, Yajima N. 2003. In vivo transgenic mutation assays. Mutat Res 540:141–151.

Tokiwa H, Otofuji T, Horikawa K, Kitamori S, Otsuka H, Manabe Y, Kinouchi T, Ohnishi Y. 1984. 1,6-Dinitropyrene: Mutagenicity in *Salmonella* and carcinogenicity in BALB/c mice. J Natl Cancer Inst 73:1359–1363.

DNA REPAIR 6 (2007) 355–366

available at www.sciencedirect.com

ScienceDirect

journal homepage: www.elsevier.com/locate/dnarepair

Replication of 2-hydroxyadenine-containing DNA and recognition by human MutSα

Flavia Barone[a], *Scott D. McCulloch*[b], *Peter Macpherson*[c], *Giovanni Maga*[d], *Masami Yamada*[e], *Takehiko Nohmi*[e], *Anna Minoprio*[a], *Filomena Mazzei*[a], *Thomas A. Kunkel*[b], *Peter Karran*[c], *Margherita Bignami*[a,*]

[a] *Unit of Experimental Carcinogenesis, Department of Environment and Primary Prevention, Istituto Superiore di Sanità, Viale Regina Elena 299, 00161 Rome, Italy*

[b] *Laboratory of Molecular Genetics and Structural Biology, National Institute of Environmental Sciences, NIH, DHHS, Research Triangle Park, North Carolina 27709, USA*

[c] *Cancer Research UK London Research Institute, Clare Hall Laboratories, South Mimms, Herts, EN6 3LD, UK*

[d] *Istituto di Genetica Molecolare, IGM-CNR, National Research Council, Via Abbiategrasso 207, 27100 Pavia, Italy*

[e] *Division of Genetics and Mutagenesis, National Institute of Health Sciences, 1-18-1 Kamiyoga, Setagaya-ku, Tokio 158-8501, Japan*

ARTICLE INFO

Article history:
Received 18 October 2006
Received in revised form
6 November 2006
Accepted 8 November 2006
Published on line 26 December 2006

Keywords:
2-Hydroxyadenine
Mismatch repair
Replication
Y family polymerases

ABSTRACT

2-Hydroxyadenine (2-OH-A), a product of DNA oxidation, is a potential source of mutations. We investigated how representative DNA polymerases from the A, B and Y families dealt with 2-OH-A in primer extension experiments. A template 2-OH-A reduced the rate of incorporation by DNA polymerase α (Pol α) and Klenow fragment (Kf^{exo-}). Two Y family DNA polymerases, human polymerase η (Pol η) and the archeal Dpo4 polymerase were affected differently. Bypass by Pol η was very inefficient whereas Dpo4 efficiently replicated 2-OH-A. Replication of a template 2-OH-A by both enzymes was mutagenic and caused base substitutions. Dpo4 additionally introduced single base deletions. Thermodynamic analysis showed that 2-OH-A forms stable base pairs with T, C and G, and to a lesser extent with A. Oligonucleotides containing 2-OH-A base pairs, including the preferred 2-OH-A:T, were recognized by the human MutSα mismatch repair (MMR). MutSα also recognized 2-OH-A located in a repeat sequence that mimics a frameshift intermediate.

1. Introduction

Reactive oxygen species (ROS) can cause oxidative damage to DNA, producing chemical changes to pyrimidine and purine bases, abasic sites and single and double strand breaks. In addition, ROS can react with the DNA precursors in the dNTP pool providing another source of oxidative DNA damage. The relative numbers of different lesions, their intrinsic miscoding potential and the efficacy of dedicated repair systems are all factors that control the final mutational load and the development of oxidation stress-related diseases. Among oxidized DNA bases, 8-oxo-7,8-dihydroguanine (8-oxoG) has attracted major attention because of its potent miscoding ability. In vitro studies have shown that template 8-oxoG can direct incorporation by DNA polymerases of either C or A [1]. The latter results in GC>TA transversions [2]. In addition, DNA polymerases can utilise 8-oxodGTP and the resulting incorporation of 8-oxoG opposite A causes AT>CG transversions

* *Corresponding author.* Tel.: +39 06 49902355; fax: +39 06 49903650.
E-mail address: bignami@iss.it (M. Bignami).

Abbreviations: ROS, Reactive oxygen species; 8-oxoG, 8-oxo-7,8-dihydroguanine; 2-OH-A, 2-hydroxyadenine; MMR, Mismatch repair; 6-FAM, 6-carboxyfluorescein; Pol α, Polymerase α; Kf^{exo-}, Klenow fragment; Dpo4, DNA polymerase 4; Pol η, Polymerase η

1568-7864/$ – see front matter © 2006 Elsevier B.V. All rights reserved.
doi:10.1016/j.dnarep.2006.11.002

and contributes to the general oxidative and mutagenic load [3,4].

In addition to 8-oxoG, sources of oxidation such as Fenton-type reagents, γ-rays or antitumor drugs [5–7] all increase the levels of 2-hydroxyadenine (2-OH-A) in DNA. 2-OH-A is also potentially miscoding [8,9]. Replication in bacteria or mammalian cells of shuttle vectors containing a single 2-OH-A produces a broader spectrum of mutations than that produced by DNA 8-oxoG [9,10]. 2-OH-A has received less attention, probably because steady-state levels of 2-OH-A residues in cellular DNA are estimated to be more than one order of magnitude lower than those of 8-oxoG ($1/10^7$ normal nucleotides) [5,6]. Significantly, the main source of DNA 2-OH-A appears to be utilization of 2-OH-dATP during replication whereas in situ oxidation of DNA adenine makes a relatively minor contribution [5]. While no information is available on the excision repair of DNA 2-OH-A, replication-related processing of 2-OH-A, including its incorporation from the oxidized dNTP pool, has been more extensively investigated. Indeed, the major replicative enzyme DNA polymerase α (Pol α) incorporated 2-OH-dATP opposite T and C in the DNA template, while *Escherichia coli* DNA polymerase I Klenow fragment (Kf^{exo-}) incorporated 2-OH-dATP only opposite T [5]. Thus, 2-OH-dATP might have a mutagenic potential for replicative DNA polymerases. It is well established that 2-OH-dATP is a substrate for hydrolysis by the human MutT homolog, hMTH1. This prevents the incorporation of 2-OH-A into DNA [11]. In addition, MYH, the MutY homolog which excises A incorporated opposite DNA 8-oxoG, also removes 2-OH-A from 2-OH-A:G base pairs. This is consistent with a role for MYH in reversing oxidation-related mismatches generated by incorporation of 2-OH-A [12].

Our previous work demonstrated that the post-replicative mismatch repair (MMR) pathway also helps to regulate the steady-state level of DNA 8-oxoG by removing the oxidized base from the nascent DNA strand [13,14]. Furthermore, overexpression of hMTH1 in MMR-defective mouse and human cells reduces the level of DNA 8-oxoG and significantly attenuates their characteristic mutator phenotype [15]. Mutation and microsatellite instability analysis indicated that a significant fraction of the oxidation-related mutations that were subject to correction by MMR occurred at A:T base pairs [15]. In particular, AT > TA, AT > GC mutations and frameshifts in runs of As were all affected. Since hMTH1 acts on both 2-OH-dATP and 8-oxodGTP [16], its expression could influence mutation by either of the oxidized purines, suggesting that DNA 2-OH-A might make a significant contribution to the mutational burden.

As a first step to clarifying the possible involvement of DNA 2-OH-A in oxidation-related mutagenesis, we have investigated some of its biochemical and physical properties. We examined the effect of 2-OH-A on replication in vitro by replicative and translesion synthesis (TLS) DNA polymerases. 2-OH-A miscoding was investigated in two unrelated DNA sequences, in A repeats or in random sequences, in which its effect on the thermal stability of DNA duplexes was quantified. The ability of a purified human MutSα DNA mismatch binding complex to recognize 2-OH-A-containing base pairs was compared in random sequences and in repetitive DNA sequences that represent frameshift intermediates. Our findings indicate that 2-OH-A is a block for replicative DNA polymerases and its bypass by TLS polymerases is mutagenic. In addition the evidence that MutSα can recognize 2-OH-A-containing base pairs, including frameshift intermediates, suggest that MMR might help to counteract the effects of 2-OH-A incorporated from the oxidized pool.

2. Materials and methods

2.1. *Oligonucleotide synthesis*

Oligonucleotides were synthesized by MWG-Biotech AG. 6-Carboxyfluorescein (6-FAM) labelled and 2-OH-A containing oligonucleotides were synthesized by the Eurogentec S.A. All oligonucleotides were further purified by denaturing polyacrylamide gels (PAGE).

2.2. *Primer extension reactions*

In standard primer extension experiments, 6-FAM labelled primers were annealed to the template strands in a 1:1 molar ratio. 6-FAM labelled DNA duplexes (50 nM) were initially pre-incubated with 0.2 pmol of mammalian Pol α in 25 mM Tris–HCl (pH 8.0), 0.5 mM DTT, 0.25 mg/ml BSA, 10 mM $MgCl_2$ buffer for 1 min. Nucleotides were then added as specified in the figure legends and the reaction continued for 10 min at 37 °C. Reactions were stopped by addition of gel loading buffer (USB Corporation) (95% formamide, 20 mM EDTA, 0.05% bromophenol blue, 0.05% xylene cyanol), the products were denatured at 95 °C for 5 min and separated on denaturing 20% PAGE. Pol α was purified from HeLa cells as described in Ref. [17]. For dNTPs incorporation and extension by Kf^{exo-} (New England Biolabs) 6-FAM labelled DNA substrates (50 nM) were incubated with the enzyme (2.5 nM) and 30 μM of each triphosphate at 37 °C in a buffer containing 20 mM Tris–HCl (pH 7.7), 2 mM $MgCl_2$, 2 mM DTT. After 0.5–5 min, an equimolar dNTP mixture was added and incubated for 5 min. Primer/template (50 nM) were pre-incubated with 150 nM DNA polymerase 4 (Dpo4), purified as described in Gruz et al. [18], at 55 °C in a buffer containing 30 mM potassium phosphate, pH 7.4, 7.5 mM $MgCl_2$, 1.25 mM β-mercaptoethanol and 5% glycerol. After 3 min the dNTP (50 μM) were added and incubated at 55 °C for 15 min. The subsequent elongation was performed by adding 50 μM of dNTPs for further 15 min. Fluorescent bands were visualized by Typhoon 9200 Gel Imager (Amersham Biosciences Europe GmbH) and quantitated by ImageQuant TL software.

2.3. *Kinetic analysis*

Experiments with Pol α, Kf^{exo-} and Dpo4 were performed under the conditions described above using 0.01–100 μM dNTP, 0.01–300 μM dNTP and 1–300 μM dNTP, respectively. Data points were derived from the analysis of the intensities of the products bands. The values of integrated gel band intensities in dependence of the nucleotide substrate concentrations ([dNTP]) were fitted to the equation:

$$I_T^*/I_{T-1} = V_{max}[dNTP]/(K_m + [dNTP])$$

where T is the target site, the template position of interest; I_T^+ = the sum of the integrated intensities at positions T, T + 1 ··· T + n.

Before being inserted in the above equation, the intensities of the single bands of interest were first normalized by dividing for the total intensity of the lane. This reduced the variability due to manual gel loading. An empty portion of the gel was scanned and the resulting value was subtracted as background. The goodness of fit of the interpolated curve was assessed by computer-aided calculation of the sum of squares of errors SSE and the correlation coefficient R^2. Interpolation, SSE, R^2 and standard errors determination were done with the computer programs GraphPadPrism and Kaleidagraph.

2.4. Bypass efficiency assay

Reaction conditions for Dpo4 and polymerase η (Pol η) were the same described previously [19]. Reaction conditions for Kf^{exo-} were as recommended by the manufacturer using 25 μM dNTPs. A truncated Pol η (residues 1–434) was overexpressed in E. coli using a modified pGEX4T3 vector that codes for a GST-Pol η fusion with a TEV cleavage site between the two proteins. Polymerase was purified by batch binding to glutathione Sepharose 4B, on-resin cleavage with TEV and MonoS column chromatography, with similar conditions to those described previously for the full length protein [20]. Dpo4 was purified as previously described [21]. The DNA substrate was a 45-mer template (5′-CCAGGTCGGTACCGGGTTAGCCTTTGGAGTCGACCTGCAGAAATT; underlined A is site of 2-OH-A) annealed to a 24-mer ^{32}P end-labelled primer (5′-AATTTCTGCAGGTCGACTCCAAAG). Reactions were prepared on ice without enzyme, preheated for 30 s to the reaction temperature, and polymerase added to initiate synthesis. Samples were removed at the indicated times, added to an equal volume of formamide loading buffer and processed as described above for analysis by 12% PAGE and scanning densitometry with a Phospholmager. All reactions contained 4 pmol substrate and the substrate:enzyme ratios: Kf^{exo-} = 1000:1, Dpo4 = 1000:1, Pol η = 750:1. Determination of single hit conditions and calculation of bypass efficiency were as described previously [21].

2.5. Bypass fidelity assay

Lesion bypass fidelity assays were performed with a substrate prepared with an unlabelled primer, using instead an internal ^{32}P-dCTP label, as described previously [21,22]. Reaction conditions were the same as for the bypass efficiency reactions, except that a 5:1 substrate:enzyme ratio was used with a 15 min incubation for all enzymes. Processing of the full length synthesis products and determination of plaque colour frequency and corresponding error rates were performed as previously described [21,22].

2.6. UV melting

Absorbance versus temperature changes were measured at 260 nm by means of a Cary 3 spectrophotometer equipped with a Peltier device for temperature control. Samples resuspended in Tris–HCl 10 mM pH 7.2, $MgCl_2$ 2 mM were placed in 1 cm path length quartz cells. The heating rate was 0.5 °C/min and data points were recorded every 0.2 °C. Absorbance values were corrected for the water thermal expansion and normalized at the absorption of 1 OD at 5 °C. Thermodynamic parameters were evaluated by extracting information by single equilibrium transition curves and data analysis was performed according to Breslauer [23].

2.7. MutSα purification and bandshift

MutSα was prepared from approximately 2×10^{10} Raji cells as previously described [24]. The final concentrated Q sepharose pool contained approximately 5 pmol MutSα per milliter. For bandshift assays, one unit of MutSα was defined as 5 fmol. Bandshift experiments were carried out with ^{32}P-end labelled oligonucleotide duplexes as previously described. Briefly, MutSα (2–10 units) was pre-incubated (5 min at 20 °C) with 2 pmol non-radioactive matched competitor duplex in 20 μl reaction buffer containing 25 mM Hepes KOH pH 8.0, 0.5 mM EDTA, 0.1 mM $ZnCl_2$, 10% glycerol, 50 μg poly(dI:dC). The 20 fmol substrate duplex was added and incubation continued for a further 20 min. Products were analysed by PAGE on 6% non-denaturing gels.

3. Results

3.1. Replication of 2-OH-A-containing templates by different DNA polymerases

Since miscoding by a DNA lesion can be influenced by the type of DNA polymerase [25,26] and the sequence context, we examined the ability of A, B and Y family DNA polymerases to bypass a template 2-OH-A in two different sequences. Because we identified oxidation-related mutations at A:T base pairs in microsatellites formed by A-runs, we placed a single 2-OH-A in the middle of an A run within a 36 mer (6A*, repeated sequence). In the second DNA substrate, a single 2-OH-A replaced the A repeat, and the 15 nt flanking sequence on both 5′ and 3′ sides was retained (A*, random sequence). In control oligonucleotides, A replaced 2-OH-A. The results obtained with each enzyme are detailed in the next sections.

3.1.1. Human DNA polymerase α

The ability of the human B family Pol α to replicate 2-OH-A located in the A* and the 6A* repeat was investigated in primer extension experiments, using primers that terminated one base immediately before the lesion (Fig. 1). Following incubation in the presence of a single dNTP, Pol α incorporated exclusively T opposite 2-OH-A in either sequence (Fig. 1A and B) and there was no detectable incorporation of any of the other three bases. Although 2-OH-A retained the coding specificity of undamaged A, its coding efficiency – the ability to instruct the polymerase to incorporate the complementary base – was significantly reduced (Fig. 1, supplementary data). The apparent incorporation efficiency (k_{cat}/K_m) for T opposite 2-OH-A was 17.5- and 5.5-fold lower than opposite A in the random and in the repeated sequence, respectively (Fig. 1C). Thus, Pol α preferentially incorporates T opposite 2-OH-A, but with

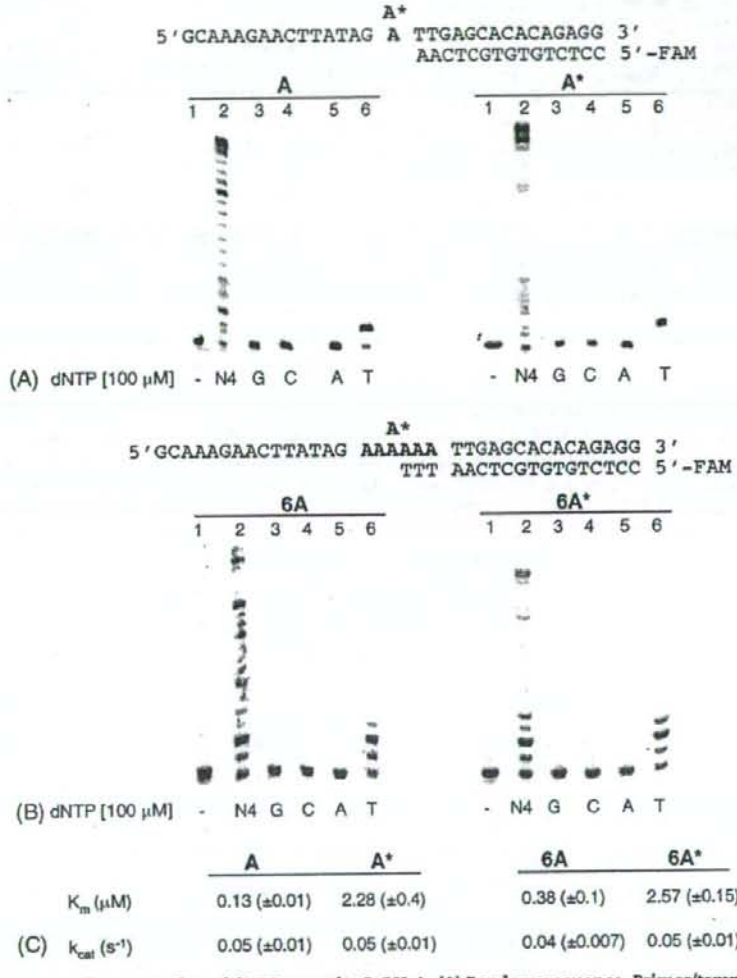

Fig. 1 – DNA polymerase α: incorporation of dNTP opposite 2-OH-A. (A) Random sequence. Primer/templates (50 nM) were pre-incubated with Pol α. After 1 min, reactions were initiated by the addition of a single triphosphate (100 μM) and continued for 10 min. Reactions products were analysed by denaturing PAGE as described in Section 2. Controls (lanes 1) were incubated without enzyme or dNTP. A* = 2-OH-A; (B) 6A or 6A* repeat sequence. The experimental conditions were the same used for the random sequence. (C) Kinetic parameters for dTTP incorporation opposite A or 2-OH-A by Pol α in the random and in the repeated sequence. K_m and k_{cat} values were evaluated as described in Section 2.

lower efficiency than opposite a normal A in both sequence contexts.

3.1.2. *E. coli DNA polymerase I (Kf^{exo-})*

In contrast to Pol α, the Klenow fragment (Kf^{exo-}) of *E. coli* DNA polymerase I is able to incorporate various bases opposite a template 2-OH-A [8]. Using the same experimental approach employed for Pol α, we compared the ability of Kf^{exo-} to replicate a template 2-OH-A in the random and in the repeated sequence. The kinetic parameters for correct and incorrect nucleotide insertion by Kf^{exo-} are summarized in Table 1A. Primer extension was observed in the presence of each of the four dNTPs but with very different efficiencies. The degree of dNTP selectivity differed for the random and the 6A* sequence. T was preferentially inserted opposite 2-OH-A in both, although the insertion efficiency was, respectively, 70- and 56-fold lower than opposite A. For the other dNTPs, the preferential order of incorporation in the A* random sequence was T ≫ G = C ≫ A with utilization of dATP three orders of magnitude lower than TTP. In the 6A* sub-

Table 1 – Kinetic parameters for dNTP incorporation opposite adenine or 2-OH-adenine by Kf^{exo-} (A) and Dpo4 (B) in a random and in a repeated sequence

A

Substrate	K_m (μM)	k_{cat} (s^{-1})	k_{cat}/K_m ($M^{-1} s^{-1} \times 10^5$)	Selectivity[a]
Kf^{exo-}				
A				
dTTP	0.0042(±0.0004)	0.6(±0.006)	1428(±14.8)	1
A*				
dTTP	0.21(±0.04)	0.43(±0.02)	20.5(±0.49)	69.7
dATP	18.1(±3.6)	0.049(±0.002)	0.03	47600
dCTP	27.7(±4.5)	0.19(±0.01)	0.67	2131
dGTP	2.1(±0.2)	0.141(±0.003)	0.7	2040
6A				
dTTP	0.06(±0.007)	1.89(±0.04)	315(±3.68)	1
6A*				
dTTP	0.55(±0.11)	0.31(±0.01)	5.6(±0.1)	56.2
dATP	4.93(±0.97)	0.04(±0.002)	0.081(±0.002)	3888.9
dCTP	13.9(±1.7)	0.039(±0.001)	0.028	11250
dGTP	3.7(±0.7)	0.036(±0.001)	0.09(±0.002)	3500

B

Substrate	K_m (μM)	k_{cat} (s^{-1})	k_{cat}/K_m ($M^{-1} s^{-1} \times 10^4$)	Selectivity[a]
Dpo4				
A				
dTTP	0.79(±0.1)	0.035	4.43	1
A*				
dTTP	11.3(±1.7)	0.017(±0.001)	0.15	29.5
dATP	85.4(±13)	0.031(±0.003)	0.03	147.7
dCTP	69.2(±11)	0.038(±0.005)	0.05	88.6
dGTP	N.D.			
6A				
dTTP	8.8(±1.4)	0.11(±0.005)	1.25	1
6A*				
dTTP	32.9(±4.5)	0.073(±0.006)	0.22	5.7
dATP	41.7(±6.5)	0.023(±0.002)	0.05	25
dCTP	N.D.[b]			
dGTP	N.D.			

[a] Selectivity is defined as $(k_{cat}/K_m)_{TTP}/(k_{cat}/K_m)_{dXTP}$, where X is A, G or C. The value represents the number of correct (TTP) incorporation events for each incorrect (dXTP) incorporation.
[b] Not detectable.

strate, the discrimination against A was relaxed and both purines were inserted with similar efficiencies and about three-fold better than C. The preferred order was T ≫ G = A > C (Table 1A).

We also examined whether Kf^{exo-} could elongate 2-OH-A-containing base pairs. Two-stage reactions were performed. In the first step, Kf^{exo-} was incubated with primer/templates and a single triphosphate to allow incorporation. To monitor the efficiency of elongation from the resulting 3′-terminal 2-OH-A base pair, a second incubation was carried out in the presence of all four dNTPs (Fig. 2, supplementary data). Kf^{exo-} efficiently elongated all terminal 2-OH-A base pairs in the random sequence. In the 6A* sequence, terminal 2-OH-A:C and 2-OH-A:A pairs impeded extension (Fig. 2, supplementary data). Similar results were obtained in an alternative approach, in which the extension of synthetic primers generating different 3′ terminal 2-OH-A-containing base pairs by Kf^{exo-} and all four dNTPs was assayed (Fig. 2A). In the 6A* sequence Kf^{exo-} efficiently elongated a terminal 2-OH-A:T or 2-OH-A:G pair whereas a 2-OH-A:A and, to a more modest extent a 2-OH-A:C pair, prevented elongation by Kf^{exo-}.

We conclude that replication of 2-OH-A by Kf^{exo-}, as with Pol α, is also relatively error-free, and T is the preferentially incorporated base. Unlike Pol α, Kf^{exo-} exhibits a somewhat more relaxed specificity and other base pairs – notably 2-OH-A: G – are also formed. Both the formation and elongation of these promutagenic base pairs is influenced by sequence context and these parameters differ significantly between the random and repeat sequence.

3.1.3. *Sulfolobus solfataricus Dpo polymerase 4*

S. solfataricus Dpo4 is an archeal Y family DNA polymerase [27]. With a single dNTP, Dpo4 inserted T, A or C opposite 2-OH-A in the A* random sequence and the preferential order of incorporation was T > C > A (Table 1B). As expected, incorporation by Dpo4 was less selective than Kf^{exo-} and dNTP utilization varied by only 3–5-fold. Surprisingly, however, addition of G was undetectable.

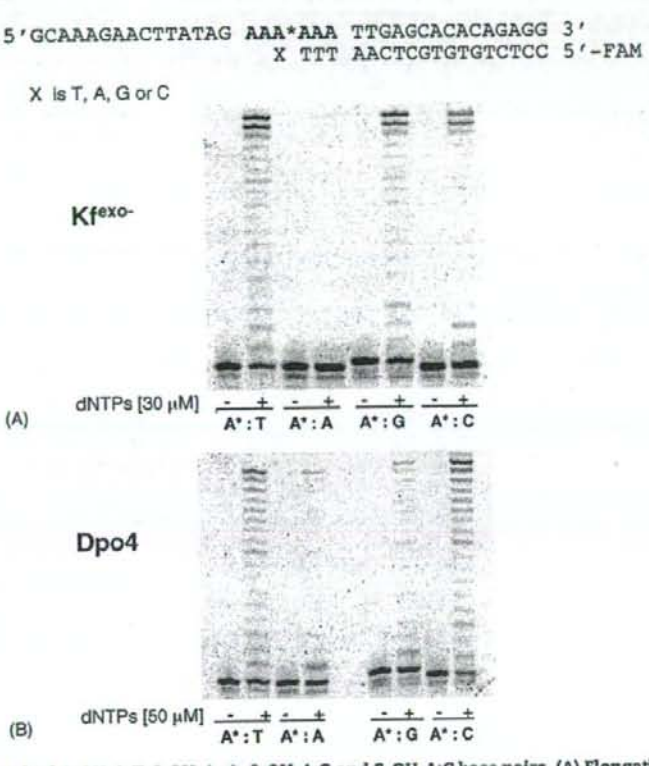

Fig. 2 – Elongation of terminal 2-OH-A:T, 2-OH-A: A, 2-OH-A:G and 2-OH-A:C base pairs. (A) Elongation of 2-OH-A containing terminal mismatches in the 6A* sequence by Kf^exo–. Reactions contained 50 nM primer/template and 2.5 nM Kf^exo– supplemented with an equimolar mixture of dNTPs (30 μM). Controls were incubated without enzyme or dNTP. (B) Elongation of 2-OH-A containing terminal mismatches in the 6A* sequence by Dpo4. Primer/template (50 nM) were pre-incubated with 150 nM Dpo4 enzyme at 55 °C for 3 min. The elongation was performed by adding 50 μM of dNTPs for 15 min.

A different result was obtained with the 6A* repeat sequence in which Dpo4 inserted predominantly T or A. Kinetic parameters indicated that T incorporation opposite 2-OH-A is only slightly lower (5.7-fold) than opposite A, while misincorporation of A is further decreased (25-fold) (Table 1B).

In this repeat sequence, Dpo4 efficiently elongated primers creating terminal 2-OH-A:T or 2-OH-A:C pairs, whereas 2-OH-A:G and 2-OH-A:A constituted a significant block (Fig. 2B). In the random sequence, none of the terminal mismatches constituted a significant block to elongation by Dpo4 (Fig. 3, supplementary data).

A template 2-OH-A in a random sequence is therefore quite efficiently bypassed by Dpo4. Bypass occurs with a significantly reduced fidelity via the formation of frequent 2-OH-A:C and 2-OH-A:A mispairs. Once formed, each of these terminal mismatches are easily elongated. Dpo4 is also considerably influenced by the sequence context of the 2-OH-A. In the 6A* repeat sequence, bypass of 2-OH-A by Dpo4 is more efficient. Its inability to extend the frequent terminal 2-OH-A:A mismatches indicates that 2-OH-A bypass in a repeat sequence is also likely to be more error free.

3.2. 2-OH-A *differentially affects the bypass efficiency of Dpo4 and human DNA polymerase η*

Bypass of 2-OH-A by Y family DNA pols was also investigated by a different approach. We used reaction conditions that reflect a single cycle of DNA synthesis with a primer terminus located such that multiple incorporations are required prior to the lesion being encountered [21]. Short incubation times and large substrate excess are chosen so that each DNA molecule is acted on only once during the time course studied. The advantage to this 'single hit' condition is that quantitative measurements of insertion efficiency opposite the lesion, extension efficiency from the damaged primer terminus and bypass efficiency (defined here as incorporation opposite at least one undamaged base beyond the lesion) can be made by comparing synthesis on the damaged and undamaged templates. All reactions described here were confirmed to be under single hit conditions that yield fainter band intensities (Fig. 3) than observed when multiple cycles of synthesis occur (Figs. 1 and supplementary data).

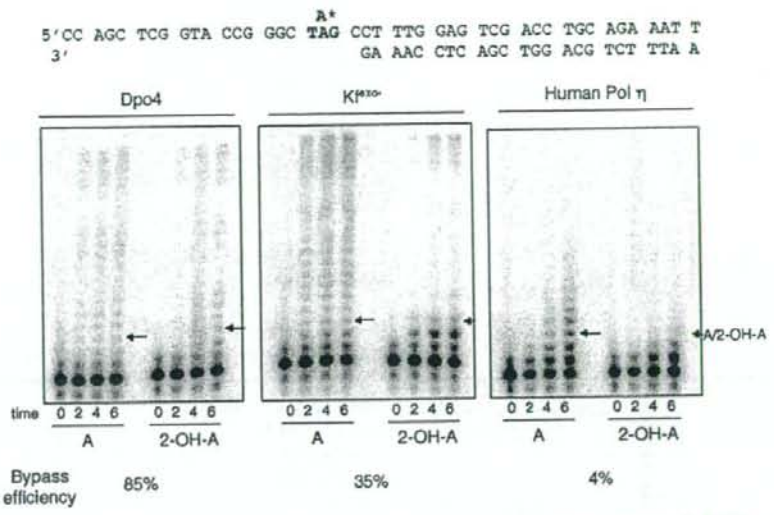

Fig. 3 – Products of 2-OH-A bypass reactions. Reactions shown are for bypass reactions with Dpo4, Kf^{exo-} and human DNA Pol η (left, middle and right panel, respectively). Each panel shows bypass of an undamaged A and 2-OH-A within a 5′-TAG substrate (as indicated in the sequence). An arrow indicates the location of the lesion.

In these assays, bypass efficiency of 2-OH-A by Dpo4 was high, 85% of the efficiency of copying the equivalent undamaged A, and there was no obvious pause at the site of the lesion (Fig. 3, arrows in left panel). The relative insertion efficiency opposite 2-OH-A and the relative extension efficiency from the damaged terminus were 79 and 88%, respectively, indicating that 2-OH-A is only a minor block to normal synthesis.

The same analysis performed with human Pol η, the prototypical Y family polymerase, indicated that bypass of 2-OH-A by this enzyme was only 4% that of undamaged A (Fig. 3, right panel). In addition, insertion opposite the lesion was also very inefficient and was only 22% of the corresponding value for A. Surprisingly, incorporation by Pol η also appeared to be inhibited at the base preceding the 2-OH-A (note the low intensity of the band immediately below the arrow in Fig. 3, right panel), a property not previously reported for this enzyme.

Kf^{exo-} was assayed under the same single hit conditions to provide a comparison (Fig. 3, middle panel). Bypass efficiency was 35% and in this case, insertion opposite the lesion (note the more intense band at the −1 position), rather than subsequent extension was particularly problematic. Both these findings are in agreement with expectations from the kinetic analysis presented in Table 1. Thus, under conditions of a single polymerase/template encounter, a template 2-OH-A lesion has a minimal impact of replication by Dpo4 whereas synthesis by human Pol η is strongly inhibited. Its overall effect on replication by Kf^{exo-} is intermediate and, as expected, the major impact is on insertion opposite the lesion.

3.3. *Fidelity of 2-OH-A bypass by Dpo4, DNA polymerase η and Kf^{exo-}*

In order to measure the error rates for a complete lesion bypass event in the presence of all four dNTPs, we used templates corresponding to the N-terminal region of the *lacZ* α-complementation gene of bacteriophage M13mp2, in which 2-OH-A (or undamaged A) is located in a TAG stop codon. Reactions designed to allow complete synthesis (to the end of the template) were carried out on all substrates and the newly synthesized strand was recovered, hybridized to gapped-duplex M13 molecules, and introduced into the appropriate *E. coli* strain [21]. Errors in synthesis at either the T, A/2-OH-A or G of the stop codon were detected as dark blue plaques and frameshift errors were detected as colourless plaques. The precise change was then identified by sequencing of mutant plaques. The frequencies of the different plaque phenotypes (Table 1, supplementary data) and the corresponding rates of base substitution and insertion/deletion errors at the lesion site are shown in Fig. 4A. Bypass of 2-OH-A by each of the three enzymes induced large increases in base substitutions (5–90 fold) relative to undamaged A, indicating 2-OH-A acts as a miscoding lesion. In addition, replication by Dpo4, but not Pol η or Kf^{exo-}, produced a six-fold increase in frameshifts at 2-OH-A. These were mostly single base deletions at the site of 2-OH-A.

Each polymerase produced a different spectrum of base substitution mutations at the 2-OH-A site (Fig. 4B). Dpo4 bypass of 2-OH-A was associated with both AT > TA transversions and AT > GC transitions (in an approximately 3:2 ratio). By contrast, bypass by Pol η caused predominantly AT > GC transitions, whereas the majority of changes for Kf^{exo-} were AT > CG transversions, with a smaller contribution from AT > TA.

These findings indicate that replication of 2-OH-A by these three polymerases is mutagenic and that the type of mutation is determined by the polymerase. Furthermore, the mutational spectra are in good general agreement with the incorporation preferences of each polymerase inferred from in vitro experi-

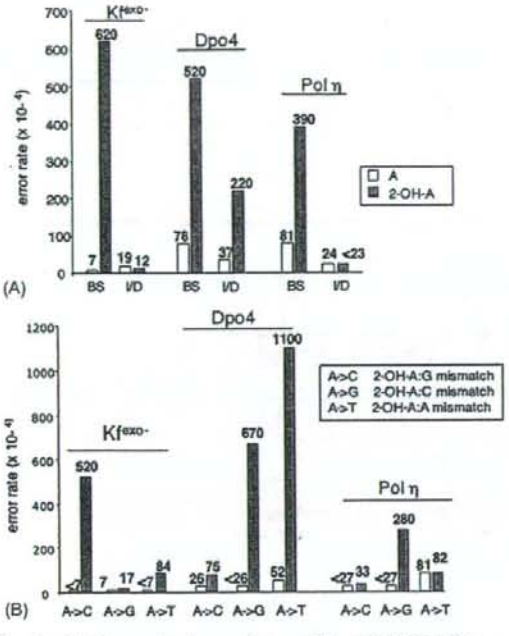

Fig. 4 – (A) Error rates for undamaged A and 2-OH-A by Dpo4, Kf^{exo-} and human DNA Pol η. The error rates of the different polymerases for undamaged A (open bars) and 2-OH-A (filled bars) are shown. BS, base substitution; I/D, insertion/deletion. (B) Base substitution error rates for Kf^{exo-}, Dpo4 and human DNA Pol η for undamaged A (open bars) and 2-OH-A (filled bars). In the box are indicated the possible 2-OH-A containing mismatches causing the observed mutations.

ments (Table 1). Interestingly, Dpo4 was the only polymerase that introduced frameshifts during replication of 2-OH-A in a non-repetitive sequence.

3.4. 2-OH-A effect on DNA secondary structure

DNA base unstacking can underlie failure in base extension during replication [28]. To determine the effects of 2-OH-A on DNA base unstacking as well as on hydrogen bond disruption we carried out thermal stability measurements on DNA duplexes containing the lesion in the random and repeated sequences (Fig. 5).

In both sequences, an A-containing mismatch produced the expected decrease in Tm (Fig. 5E and F). Replacement of A:T by 2-OH-A:T produced only minor changes in the thermal and thermodynamic stability of either the repeat or random duplexes (Fig. 5A and B). In the random sequence 2-OH-A caused a slight destabilization (Fig. 5B), whereas it had the opposite effect in the repeat sequence (Fig. 5A). 2-OH-A:C or 2-OH-A:G mismatches were without detectable effect and Tm differences in comparison to 2-OH-A:T were within the limits of experimental error (Fig. 5C and D).

The data indicate that 2-OH-dA can form stable base pairs with T and that the sequence context has a role in stacking optimization with stacking favoured in a repetitive A sequence. In contrast to unmodified A, pairing of 2-OH-A with the other bases, with a single exception of A, are relatively favoured. The adoption of a more suitable tautomeric form of the 2-OH-A in base pairs might be responsible for this effect [29].

3.5. Recognition by the hMutSα complex of 2-OH-A containing DNA

Because oxidation-related frameshifts at A repeat sequences are influenced by MMR [15], we examined whether purified MutSα recognizes 2-OH-A-containing base pairs. Duplexes based on the 6A* oligonucleotide in which the 2-OH-A strand was annealed to a complementary strand containing 6, 5 or 7 Ts opposite the A6 sequence were used as substrates for binding by MutSα. These represent frameshift intermediates with an insertion/deletion loop of one base. Band-shift analysis indicated that neither the 2-OH-A:T base pair in the 6A*:6T duplex nor an A:T pair in the control duplex was recognized by MutSα (Fig. 6A). In contrast, we observed significant binding to a duplex containing an extra A in the 2-OH-A-containing strand (6A*:5T). Comparable binding was observed to the duplex in which an extra T was positioned opposite the 2-OH-A-containing strand (6A*:7T) (Fig. 6A). In each case, binding was similar to that observed with duplexes containing either an extra unmodified A or T.

In a second series of experiments, we examined binding to 2-OH-A-containing base pairs in non-repetitive sequences. In this case, 2-OH-A provoked significant recognition by MutSα. Of particular note, binding to a 2-OH-A:T base pair was comparable to that seen with other 2-OH-A-containing mispairs (Fig. 6B). Under the same experimental conditions, there was no detectable binding by MutSα to the control A:T duplex. Recognition of a 2-OH-A:T base pair was also observed with a second series of duplexes based on an unrelated random sequence (data not shown).

These findings indicate that MMR might be engaged at 2-OH-A base pairs. MutSα recognition of 2-OH-A-containing structures resembling slipped-mispaired intermediates suggests a role in counteracting frameshifts caused by these oxidized bases in repetitive sequences. In addition, the ability of MutSα to recognize 2-OH-A containing mispairs is consistent with an involvement in suppressing base substitution mutations caused by oxidatively damaged adenine.

4. Discussion

Our previous analysis of oxidation-related spontaneous mutations in MMR deficient cells identified 2-OH-A as a potentially significant contributor to several classes of mutation [15]. Since these included frameshifts in A runs as well as base substitutions, we investigated some of the structural and biological properties of this oxidized purine in repetitive and non repetitive DNA sequence contexts.

Our findings indicate that incorporation opposite 2-OH-A is difficult for both the A family Kf^{exo-} DNA polymerase and

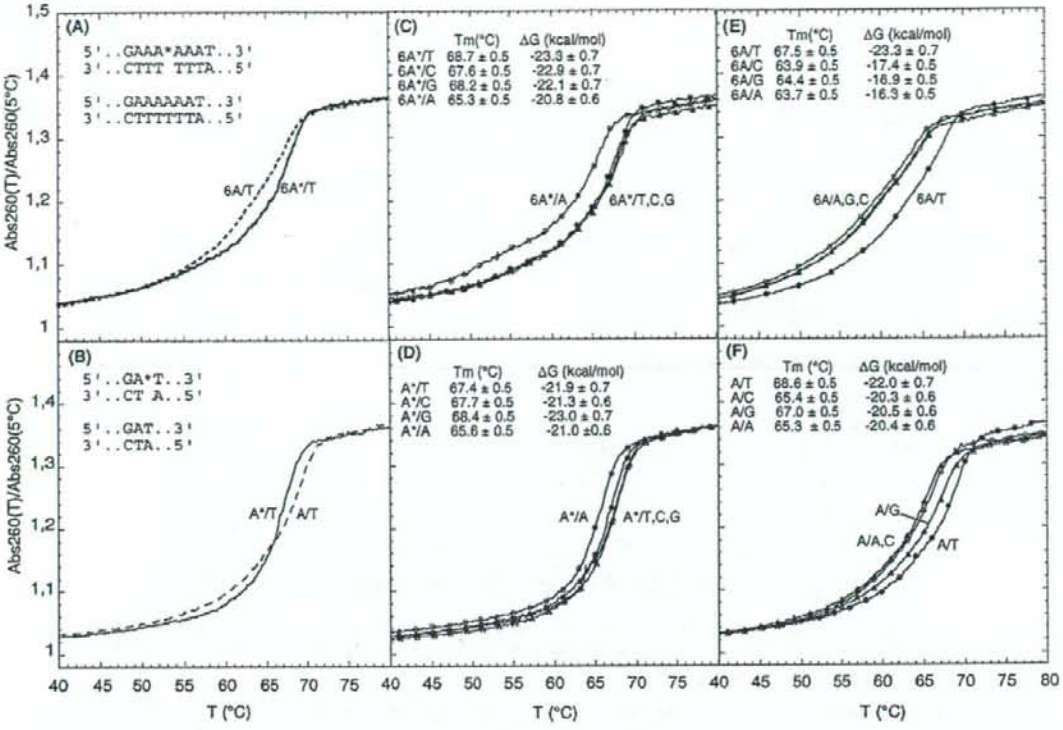

Fig. 5 – UV denaturation profiles of DNA duplexes with and without 2-OH-A. Effect of 2-OH-A:T pairing in the 6A repeat sequence (panel A) and in a random sequence (panel B); continuous line, 2-OH-A:T; dashed line, A:T. Thermal stability of DNA duplexes with A or 2-OH-A paired with T, G, C or A in the A-repeat sequence (panels E and C, respectively) and in the random sequence (panels F and D). Filled circle, A:T and 2-OH-A:T; empty circle, A:A and 2-OH-A:A; filled triangle, A:C and 2-OH-A:C; empty triangle, A:G and 2-OH-A:G.

the B family replicative Pol α. This distinguishes 2-OH-A from 8-oxoG, which is easily bypassed by several replicative polymerases via the mutagenic incorporation of an A opposite the lesion [1]. Thus, unlike 8-oxo-G, a template 2-OH-A might cause a permanent or transient replication block thereby provoking recruitment of a TLS polymerase. Among the enzymes we tested, Dpo4 was the least sensitive to 2-OH-A, while human Pol η was inefficient in bypassing the lesion. This raises the possibility that of the human Y family polymerases the Dpo4 homolog, polymerase κ, rather than Pol η, might be better equipped to bypass this oxidized purine. The different efficiencies of 2-OH-A bypass by Dpo4 and Pol η resemble their behaviour with AP sites and may reflect differences in their respective "little finger" subdomains [30,31], probably the critical features that allow lesion bypass [21].

Each polymerase showed a strong preference for insertion of T opposite 2-OH-A although our incorporation data suggested a range of alternative permissible base pairings that were affected by the sequence context of the oxidized base. These findings are consistent with the known ability of DNA 2-OH-A to adopt multiple tautomeric forms that are influenced by temperature, solvent polarity and neighbouring bases [32–34]. In particular, a shift from the prevailing keto tautomer (N1-H) towards the enol form (O2H) is likely to affect the probability that the lesion is accommodated as 2-OH-A:T or with other partners through classical W–C bonding or wobble base pairs. They are also consistent with our Tm measurements, which indicated that 2-OH-A forms stable base pairs not only with T, but also with C or G. Thus, the different abilities of DNA polymerases to accommodate otherwise unfavourable 2-OH-A tautomers within their active sites might influence replication fidelity [35].

A previous investigation of mutational spectra in MMR-defective cells indicated that AT>GC and AT>TA base substitutions (and to a minor extent AT>CG) might derive from miscoding by an oxidized purine [15]. These were the most frequent mutations observed following replication of 2-OH-A by Dpo4 and Pol η under conditions of limited polymerase engagement. The same analysis also revealed that frameshifts, with deletion of the 2-OH-A adduct, were significantly increased following replication by Dpo4. This

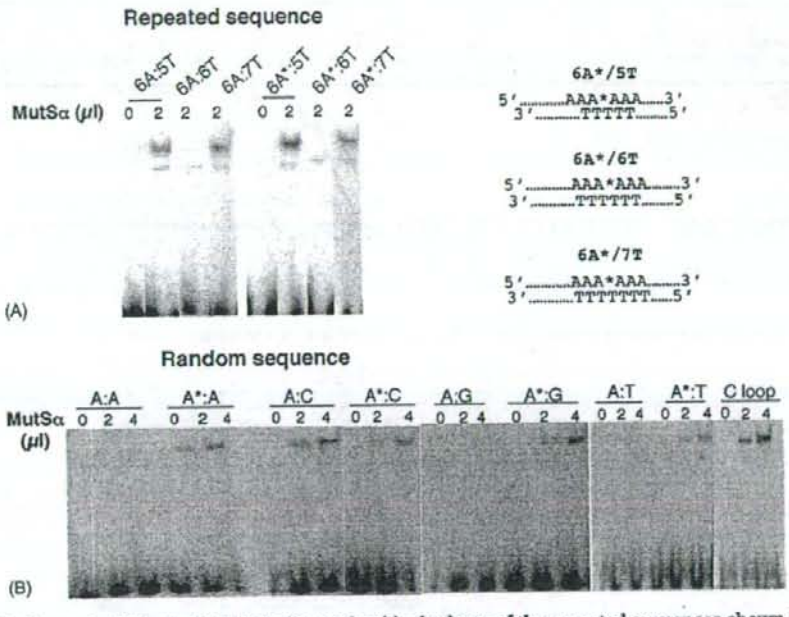

Fig. 6 – MutSα binding to 2-OH-A. End-labelled oligonucleotide duplexes of the repeated sequences shown in panel A were incubated with MutSα. In panel B is shown MutSα binding to 2-OH-A in random sequences. Products were analysed by non-denaturing PAGE as described in Section 2.

polymerase has a very low frameshift fidelity, which is consistent with its ability to accommodate unpaired nucleotides in the active site [30]. It is also known to generate deletions at noniterated nucleotides [36]. Together with the apparent difficulties experienced by replicative polymerases at a template 2-OH-A, these findings strengthen the likelihood that Y polymerase-mediated TLS occurs at this lesion.

Little or no information is available on the repair of 2-OH-A formed by in situ oxidation of DNA adenine. We show here that the major human MMR recognition complex, MutSα, recognizes 2-OH-A-containing oligonucleotides. Recognition by MutSα was context dependent. MutSα efficiently recognized oligonucleotide duplexes containing 2-OH-A in structures mimicking insertion/deletion loop (IDL) within a 6A repeat. In this regard, the behaviour of the oxidized adenine was indistinguishable from its normal homolog. Within the same type of IDL structure, the behaviour of 2-OH-A differs from DNA 8-oxoG, which appears to assume a conformation that renders it invisible to MutSα [37]. The ability of MutSα to recognize 2-OH-A within an IDL context may have relevance in vivo as it is consistent with the apparent contribution of the oxidized base to microsatellite instability at the A_{26} BAT26 sequence in MMR-defective cells [15].

Although duplexes containing 8-oxoG:C base pairs are not recognized [38,39], MutSα bound each of the four 2-OH-A-containing base pairs to a similar extent. Alterations in base geometry and local flexibility are likely to be major determinants of mismatch recognition [28,40]. Recognition of 2-OH-A:T pairs might again reflect the unique ability of 2-OH-A to adopt multiple tautomeric forms, some of which are associated with wobble base pairs and local distortion [33]. A 2-OH-A:T pair in a fully paired A6 repeat sequence was not recognized by MutSα, however. A_n repeats of this kind are known to assume unusual conformations in which the A:T base pairs show large propeller twist angles and form bifurcated hydrogen bonds involving the N6 amino group of A and the O4 atoms of two adjacent Ts in the opposite strand. We speculate that this particular structural arrangement might confer a greater resistance to deformation and thereby prevent DNA from adopting the structural changes needed to trigger MutSα recognition.

Notwithstanding the precise mechanism by which MutSα recognizes 2-OH-A-containing base pairs, our findings clearly indicate how MMR might help control the steady-state levels of DNA 2-OH-A. The major source of DNA 2-OH-A is acknowledged to be the oxidized dNTP pool [5]. MMR would reverse this incorporation and prevent the accumulation of 2-OH-A in DNA. This role is consistent with the higher levels of DNA 2-OH-A observed in $msh2^{-/-}$ ES cells in comparison to wild type ES cells [41].

In summary, we have shown that replication fork block is the likely outcome of a replicative DNA polymerase encountering a template 2-OH-A. Our findings indicate that a specialized bypass polymerase might overcome the block at the expense of replication fidelity. In addition, MutSα recognition of 2-OH-A-containing substrates indicates that MMR might contribute to mutation avoidance by acting on 2-OH-A-containing base pairs.

Acknowledgements

This work has been partially supported by grants from AIRC, ISS/NIH, FIRB to MB, by the Intramural Research Program of the NIH, National Institute of Environmental Health Sciences to TK, from a grant-in-aid for international collaborative research SH34407 (Japan Health Science Foundation) to MY and MB, by the CARIPLO Foundation project "Oncogenetica e Proteomica della Replicazione" (2003.1663/10.8441) to GM. We would like to thank Dr. Lars Pedersen of the NIEHS for construction and purification of Pol η.

Appendix A. Supplementary data

Supplementary data associated with this article can be found, in the online version, at doi:10.1016/j.dnarep.2006.11.002.

REFERENCES

[1] S. Shibutani, M. Takeshita, A.P. Grollman, Insertion of specific bases during DNA synthesis past the oxidation-damaged base 8-oxodG, Nature 349 (1991) 431–434.
[2] K.C. Cheng, D.S. Cahill, H. Kasai, S. Nishimura, L.A. Loeb, 8-Hydroxyguanine, an abundant form of oxidative DNA damage, causes G>T and A>C substitutions, J. Biol. Chem. 267 (1992) 166–172.
[3] Y.I. Pavlov, D.T. Minnick, S. Izuta, T.A. Kunkel, DNA replication fidelity with 8-oxodeoxyguanosine triphosphate, Biochemistry 33 (1994) 4695–4701.
[4] M. Inoue, H. Kamiya, K. Fujikawa, Y. Ootsuyama, N. Murata-Kamiya, T. Osaki, K. Yasumoto, H. Kasai, Induction of chromosomal gene mutations in *Escherichia coli* by direct incorporation of oxidatively damaged nucleotides. New evaluation method for mutagenesis by damaged DNA precursors in vivo, J. Biol. Chem. 273 (1998) 11069–11074.
[5] H. Kamiya, H. Kasai, Formation of 2-hydroxydeoxyadenosine triphosphate, an oxidatively damaged nucleotide, and its incorporation by DNA polymerases. Steady-state kinetics of the incorporation, J. Biol. Chem. 270 (1995) 19446–19450.
[6] S. Frelon, T. Douki, J. Cadet, Radical oxidation of the adenine moiety of nucleoside and DNA: 2-hydroxy-2′-deoxyadenosine is a minor decomposition product, Free Radic. Res. 36 (2002) 499–508.
[7] M. Birincioglu, P. Jaruga, G. Chowdhury, H. Rodriguez, M. Dizdaroglu, K.S. Gates, DNA base damage by the antitumor agent 3-amino-1,2,4-benzotriazine 1,4-dioxide (tirapazamine), J. Am. Chem. Soc. 125 (2003) 11607–11615.
[8] H. Kamiya, T. Ueda, T. Ohgi, A. Matsukage, H. Kasai, Misincorporation of dAMP opposite 2-hydroxyadenine, an oxidative form of adenine, Nucleic Acids Res. 23 (1995) 761–766.
[9] H. Kamiya, H. Kasai, Mutations induced by 2-hydroxyadenine on a shuttle vector during leading and lagging strand synthesis in mammalian cells, Biochemistry 36 (1997) 11125–11130.
[10] H. Kamiya, H. Kasai, Substitution and deletion mutations induced by 2-hydroxyadenine in *Escherichia coli*: effects of sequence contexts in leading and lagging strands, Nucleic Acids Res. 25 (1997) 304–311.
[11] K. Fujikawa, H. Kamiya, H. Yakushiji, Y. Fujii, Y. Nakabeppu, H. Kasai, The oxidized forms of dATP are substrates for the human MutT homologue, the hMTH1 protein, J. Biol. Chem. 274 (1999) 18201–18205.
[12] Y. Ushijima, Y. Tominaga, T. Miura, D. Tsuchimoto, K. Sakumi, Y. Nakabeppu, A functional analysis of the DNA glycosylase activity of mouse MUTYH protein excising 2-hydroxyadenine opposite guanine in DNA, Nucleic Acids Res. 33 (2005) 672–682.
[13] C. Colussi, E. Parlanti, P. Degan, G. Aquilina, D. Barnes, P. Macpherson, P. Karran, M. Crescenzi, E. Dogliotti, M. Bignami, The mammalian mismatch repair pathway removes DNA 8-oxodGMP incorporated from the oxidized dNTP pool, Curr. Biol. 12 (2002) 912–918.
[14] M.T. Russo, G. De Luca, P. Degan, M. Bignami, Different DNA repair strategies to combat the threat from 8-oxoguanine, Mutat. Res. (10) (2006) (Epub ahead of print).
[15] M.T. Russo, M.F. Blasi, F. Chiera, P. Fortini, P. Degan, P. Macpherson, M. Furuichi, Y. Nakabeppu, P. Karran, G. Aquilina, M. Bignami, The oxidized deoxynucleoside triphosphate pool is a significant contributor to genetic instability in mismatch repair-deficient cells, Mol. Cell. Biol. 24 (2004) 465–474.
[16] K. Sakumi, M. Furuichi, T. Tsuzuki, T. Kakuma, S. Kawabata, H. Maki, M. Sekiguchi, Cloning and expression of cDNA for a human enzyme that hydrolyzes 8-oxo-dGTP, a mutagenic substrate for DNA synthesis, J. Biol. Chem. 268 (1993) 23524–23530.
[17] T. Weiser, M. Gassmann, P. Thommes, E. Ferrari, P. Hafkemeyer, U. Hubscher, Biochemical and functional comparison of DNA polymerases alfa, delta and epsilon from calf thymus, J. Biol. Chem. 266 (1991) 10420–10428.
[18] P. Gruz, F.M. Pisani, M. Shimizu, M. Yamada, I. Hayashi, K. Morikawa, T. Nohmi, Synthetic activity of Sso DNA polymerase Y1, an archaeal DinB-like DNA polymerase, is stimulated by processivity factors proliferating cell nuclear antigen and replication factor C, J. Biol. Chem. 276 (2001) 47394–47401.
[19] S.D. McCulloch, R.J. Kokoska, C. Masutani, S. Iwai, F. Hanaoka, T.A. Kunkel, Preferential cis-syn thymine dimer bypass by DNA polymerase eta occurs with biased fidelity, Nature 428 (2004) 97–100.
[20] T. Matsuda, K. Bebenek, C. Masutani, I.B. Rogozin, F. Hanaoka, T.A. Kunkel, Error rate and specificity of human and murine DNA polymerase eta, J. Mol. Biol. 312 (2001) 335–346.
[21] R.J. Kokoska, S.D. McCulloch, T.A. Kunkel, The efficiency and specificity of apurinic/apyrimidinic site bypass by human DNA polymerase eta and *Sulfolobus solfataricus* Dpo4, J. Biol. Chem. 278 (2003) 50537–50545.
[22] S.D. McCulloch, T.A. Kunkel, Measuring the fidelity of translesion DNA synthesis, Methods Enzymol. 408 (2006) 341–355.
[23] K.J. Breslauer, Extracting thermodynamic data from equilibrium melting curves for oligonucleotide order-disorder transitions, in: S. Agraval (Ed.), Methods in Molecular Biology, vol. 26, Humana Press Inc., Totowa, NJ, 1994, pp. 347–372.
[24] P. Macpherson, O. Humbert, P. Karran, Frameshift mismatch recognition by the human MutS alpha complex, Mutat. Res. 408 (1998) 55–66.
[25] S. Prakash, R.E. Johnson, L. Prakash, Eukaryotic translesion synthesis DNA polymerases: specificity of structure and function, Annu. Rev. Biochem. 74 (2005) 317–353.
[26] T.A. Kunkel, DNA replication fidelity, J. Biol. Chem. 279 (2004) 16895–16898.
[27] H. Ohmori, E.C. Friedberg, R.P. Fuchs, M.F. Goodman, F. Hanaoka, D. Hinkle, T.A. Kunkel, C.W. Lawrence, Z. Livneh, T. Nohmi, L. Prakash, S. Prakash, T. Todo, G.C. Walker, Z. Wang, R. Woodgate, The Y-family of DNA polymerases, Mol. Cell 8 (2001) 7–8.

[28] W. Yang, Poor base stacking at DNA lesions may initiate recognition by many repair proteins, DNA Repair 5 (2006) 654–666.
[29] J. Kawakami, H. Kamiya, K. Yasuda, H. Fujiki, H. Kasai, N. Sugimoto, Thermodynamic stability of base pairs between 2-hydroxyadenine and incoming nucleotides as a determinant of nucleotide incorporation specificity during replication, Nucleic Acids Res. 29 (2001) 3289–3296.
[30] H. Ling, F. Boudsocq, R. Woodgate, W. Yang, Crystal structure of a Y-family DNA polymerase in action: a mechanism for error-prone and lesion-bypass replication, Cell 107 (2001) 91–102.
[31] J. Trincao, R.E. Johnson, C.R. Escalante, S. Prakash, L. Prakash, A.K. Aggarwal, Structure of the catalytic core of *S. cerevisiae* DNA polymerase eta: implications for translesion DNA synthesis, Mol. Cell 8 (2001) 417–426.
[32] J. Sepiol, Z. Kazimierczuk, D. Shugar, Tautomerism of isoguanosine and solvent-induced keto-enol equilibrium, Z Naturforsch [C] 31 (1976) 361–370.
[33] H. Robinson, Y.G. Gao, C. Bauer, C. Roberts, C. Switzer, A.H. Wang, 2′-Deoxyisoguanosine adopts more than one tautomer to form base pairs with thymidine observed by high-resolution crystal structure analysis, Biochemistry 37 (1998) 10897–10905.
[34] A.M. Maciejewska, K.D. Lichota, J.T. Kusmierek, Neighbouring bases in template influence base-pairing of isoguanine, Biochem. J. 369 (2003) 611–618.
[35] J.R. Bias, F.J. Luque, M. Orozco, Unique tautomeric properties of isoguanine, J. Am. Chem. Soc. 126 (2004) 154–164.
[36] R.J. Kokoska, K. Bebenek, F. Boudsocq, R. Woodgate, T.A. Kunkel, Low fidelity DNA synthesis by a y family DNA polymerase due to misalignment in the active site, J. Biol. Chem. 277 (2002) 19633–19638.
[37] P. Macpherson, F. Barone, G. Maga, F. Mazzei, P. Karran, M. Bignami, 8-oxoguanine incorporation into DNA repeats in vitro and mismatch recognition by MutSalpha, Nucleic Acids Res. 33 (2005) 5094–5105.
[38] A. Mazurek, M. Berardini, R. Fishel, Activation of human MutS homologs by 8-oxoguanine DNA damage, J. Biol. Chem. (2001) [Epub].
[39] E.D. Larson, K. lams, J.T. Drummond, Strand-specific processing of 8-oxoguanine by the human mismatch repair pathway: inefficient removal of 8-oxoguanine paired with adenine or cytosine, DNA Repair (Amst) 2 (2003) 1199–1210.
[40] T.A. Kunkel, D.A. Erie, DNA mismatch repair, Annu. Rev. Biochem. 74 (2005) 681–710.
[41] T.L. DeWeese, J.M. Shipman, N.A. Larrier, N.M. Buckley, L.R. Kidd, J.D. Groopman, R.G. Cutler, H. te Riele, W.G. Nelson, Mouse embryonic stem cells carrying one or two defective Msh2 alleles respond abnormally to oxidative stress inflicted by low-level radiation, Proc. Natl. Acad. Sci. U.S.A. 95 (1998) 11915–11920.